# A 5 Hz flashlamp pumped Cr:LiSAF multipass amplifier for ultrashort pulses

## R E Samad, G E C Nogueira, S L Baldochi and N D Vieira Jr

Centro de Lasers e Aplicações, Instituto de Pesquisas Energéticas e Nucleares,
IPEN–CNEN/SP Avenida Professor Lineu Prestes, 2242, Cidade Universitária,
CEP 05508-000, São Paulo, SP, Brazil

E-mail: resamad@gmail.com

**Abstract**
We report here the operation, at 5 Hz, of a multipass flashlamp pumped Cr:LiSAF ultrashort
pulse amplifier, presenting peak powers over 0.3 TW. This unusual high repetition rate was
obtained by using a two-flashlamp pumping scheme, aiming at the minimization of the thermal
load on the gain medium by the use of intracavity absorption filters. This cavity was used as a
four-pass multipass amplifier in a hybrid Ti:sapphire/Cr:LiSAF system. The maximum
amplification factor was 150, and the compressed pulse duration was 60 fs.

(Some figures in this article are in colour only in the electronic version)

## 1. Introduction

Cr:LiSAF ($Cr^{3+}$:LiSrAlF$_6$) single crystals are very attractive
gain media due to their spectroscopic properties [1], such as
a long lifetime of the upper laser level at room temperature
($\sim$67 $\mu$s) [2], three broad absorption bands [2], a wide
emission band ranging from 650 to 1050 nm, and a high
saturation fluence. Laser action has been demonstrated under
several pumping schemes [2–6], and pulse durations down to
a few femtoseconds in mode-locking regime [7] have been
achieved. The Cr:LiSAF wide emission band, theoretically
capable of supporting ultrashort pulses shorter than 5 fs, make
it suitable for the generation and amplification of ultrashort
pulses. Besides, the long lifetime of the laser transition is an
advantage when compared to Ti:sapphire, because it results in
a higher saturation fluence (greater energy storage capability),
and allows the crystal to be flashlamp pumped (or even battery
fed diode pumped [5]) instead of requiring another laser.

Flashlamp pumped Cr:LiSAF lasers [3, 8–10] have been
developed reaching pulse energies up to 8.8 J and average
powers up to 4.5 W [8], and flashlamp pumped ultrashort
pulse amplifiers [10–13] have achieved peak powers up to
8.5 TW. Regrettably, the LiSAF host has poor thermal
properties [14] that include a low thermal conductivity and a
strong temperature dependence of the laser transition lifetime
due to thermal quenching [15], limiting the operation repetition
rate of flashlamp pumped Cr:LiSAF lasers below 12 Hz [8] and
of TW level amplifiers under 1 Hz [10–13, 16–18]. In a gain
medium in the shape of a rod, crystal cracking due to thermally
induced stress was reported at 18 Hz [19].

The main heat source in a flashlamp pumped Cr:LiSAF
crystal is the Stokes shift from the three absorption bands
centred at 290, 450 and 650 nm to the emission band at 830 nm.
To reduce this thermal load on the Cr:LiSAF rod, we developed
and built a two-flashlamp pumping cavity with intracavity
filters that select the absorption bands being pumped, allowing
a certain degree of control over the heat being generated
inside the gain medium. We demonstrated that this scheme
allowed the laser operation at repetition rates as high as 30 Hz
with 20 W of average power [20], or 15 Hz with 30 W of
average power [21], depending on the filters used. Here we
report results obtained when using this pumping cavity as an
ultrashort pulse amplifier in a multipass configuration.

## 2. Experimental setup

The pumping cavity houses two xenon flashlamps, a
1.5 mol% Cr doped Cr:LiSAF rod (101.6 mm long, 6.35 mm
diameter) with Brewster angled faces. Absorption filters are
placed between each lamp and the rod. Each flashlamp is

individually fed by a power supply that can deliver up to 50 J of electrical energy in 65 $\mu$s pulses. The design details have been given in our previous work [20]. To operate as an ultrashort pulse amplifier, the pumping cavity was added to a CPA [22] system comprising a Ti:sapphire main oscillator (Mira-Seed, Coherent) that generates ∼20 nm, 50 fs ultrashort pulses (not transform limited at the oscillator output), and a Ti:sapphire multipass amplifier (Odin, Quantronix) that stretches, amplifies and compresses the output pulses to ∼1 mJ at 1 kHz repetition rate. The compressed pulses' duration can be adjusted to a minimum of ∼40 fs full-width at half-maximum (FWHM) by changing the distance between the compressor gratings. The Odin amplifier has a 1 ps nm$^{-1}$ stretcher, and was modified to allow the extraction of the amplified, uncompressed pulses (∼20 ps FWHM), that were injected into the Cr:LiSAF rod for amplification. After amplification, an external high-energy temporal compressor matched to the Odin stretcher compressed the amplified pulses, which were then characterized by a single-shot autocorrelator (SSA, Coherent).

## 3. Results

For the initial measurements, a set of filters that allow pumping only in the 650 nm band (filter set 1 of our earlier work [21]) was used inside the pumping cavity. These filters minimize the thermal load on the gain medium, allowing operation at high repetition rates [20]. The Ti:sapphire amplified, ∼20 ps stretched pulses were injected into the Cr:LiSAF crystal under pumping, and the amplification $\mathcal{A}$, defined by the ratio between the pulse energies that emerge from the Cr:LiSAF under pumping and without pumping, was measured after one pass through the rod, at 1 Hz repetition rate. To ensure that the energy measured was from the amplified pulses and not from the Cr:LiSAF spontaneous emission, an iris was placed between the Cr:LiSAF rod and the energy meter (allowing the laser beam to go through it), and it was positioned in such a way that, when the pulses were blocked before the amplifier, no energy was measured when the flashlamps were triggered. The results are shown as filled circles in figure 1, where it can be seen that the amplification grows linearly with the pumping power, indicating a low gain regime, and the maximum amplification was just over 1.5 per pass. This value, although suitable for a regenerative amplifier, is too low for a multipass configuration. To increase the gain per pass we investigated the amplification behaviour when using the two other filter sets of our earlier work [21], and the results are also shown in figure 1. In this graph, the hollow triangles represent the gain when pumping the 650 and the 450 nm bands (filter set 2 [21]), providing a gain that increases exponentially with the pumping energy (high gain system), that reaches a maximum value of 2.7 under 100 J pumping. In the same graph, the hollow squares are the results when pumping the 650 and 450 nm bands and also the wing of the 290 nm band (filter set 3 [21]), also showing an exponential gain with the pumping energy, and the maximum amplification is $3.61 \pm 0.09$ per pass. This higher amplification regime was chosen as adequate for the multipass amplifier.
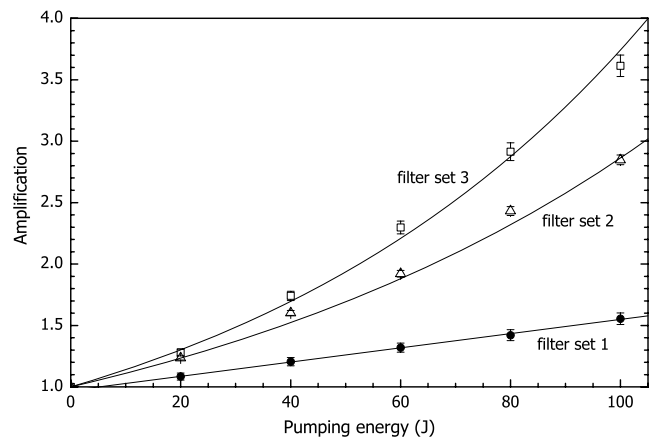


**Figure 1.** Pulse amplification dependence on the pumping energy. When pumping only on the 650 nm absorption band (filled circles), the amplification is linear. Exponential amplification is observed when also pumping the 450 nm band (hollow triangles) and the wing of the 290 nm absorption band (hollow squares).

The spatial profile of the laser beam amplified by a single pass through the Cr:LiSAF rod was measured after 1 m of propagation in free space, with and without pumping, for the intracavity filter set 2 (that allowed pumping in the 450 and 650 nm bands), using a 640 × 480 pixels CCD camera (Newport LBP-2). Figure 2(a) shows the beam spatial profile without pumping, in a false colour scheme; the white lines intersect at the beam peak intensity position, and the intensity profiles along these lines are show at the bottom and at the right of this figure. Figure 2(b) presents these normalized horizontal and vertical peak intensity profiles measured without pumping and under 20, 60 and 100 J pumping. Although the distance from the rod to the CCD camera is not enough to assure a far-field measurement that would allow small wavefront (phase) distortions accumulated inside the gain media to modify the beam spatial distribution, it can be clearly seen that there are no major distortions on the intensity profiles. This shows that the gain distribution inside the Cr:LiSAF crystal is homogeneous, and the amplification keeps the beam profile. Although these beam spatial profile measurements were made for filter set 2 and we opted to use filter set 3 [21] for the multipass amplifier, the small wing of the 290 nm absorption band being pumped in the later case should not introduce significant changes in the Cr:LiSAF rod gain homogeneity.

Having established that the intracavity filter set 3 provides the gain needed for the multipass amplifier configuration due to the pumping in the three absorption bands [21], the double-pass amplification was measured as a function of the pumping energy. Figure 3 shows the double-pass amplification results (filled circles), at 2 Hz repetition rate, together with the square of the single-pass amplification, and the good agreement between these data evidences that no intensity-dependent (nonlinear) losses were inserted in the second pass, and that the 2 Hz amplification reproduces the 1 Hz values. The maximum amplification measured was $13.4 \pm 0.7$ at 100 J pumping energy.

We proceeded to determine the double-pass amplification dependence on the repetition rate, and the 1 Hz amplification
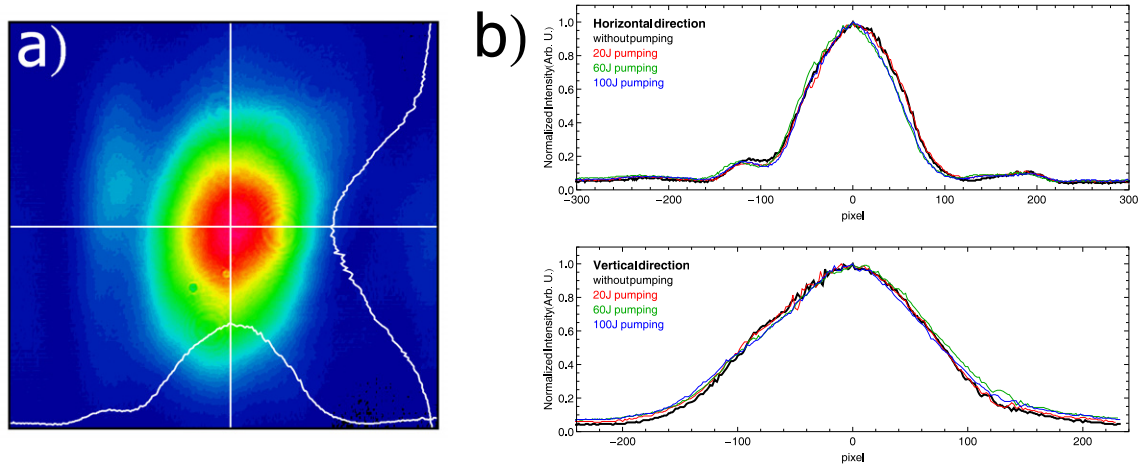
**Figure 2.** (a) Beam profile before amplification by the Cr:LiSAF crystal, showing the peak intensity profiles. (b) Peak intensity profiles for the beam before amplification (thicker line) and under 20, 60 and 100 J pumping (thinner lines).
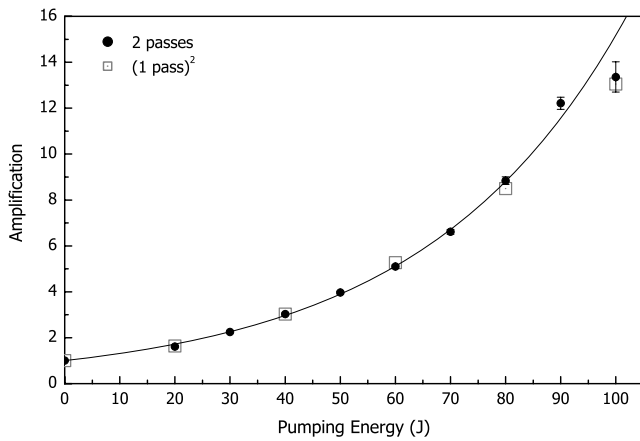


**Figure 3.** Double-pass amplification for 20 ps pulses, at 2 Hz repetition rate (filled circles), fitted by an exponential function.
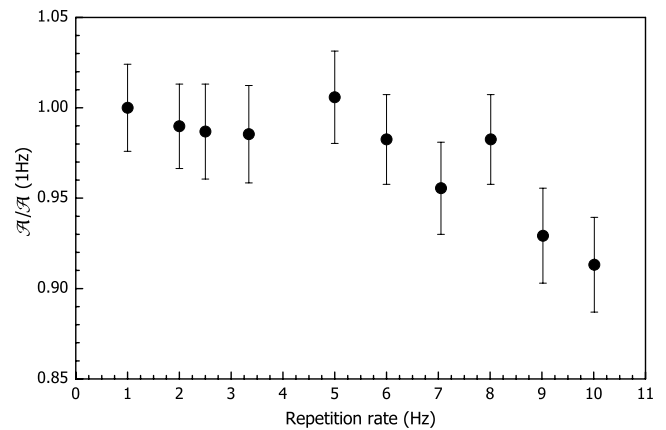


**Figure 4.** Double-pass pulse amplification as a function of the repetition rate. The amplification $\mathcal{A}$ is normalized by the 1 Hz amplification $\mathcal{A}$ (1 Hz).

normalized results are depicted in figure 4. This figure shows that the amplification is constant (within experimental error) up to 5 Hz, dropping for higher repetition rates, demonstrating that our scheme to reduce the thermal load on the Cr:LiSAF rod that improved the laser performance [21] can also be used to increase the repetition rate of Cr:LiSAF flashlamp pumped ultrashort pulse amplifiers. This amplification decrease is consistent with the behaviour observed when operating the pumping cavity as a laser (inside a resonator) with filter set 3 [20], and is attributed to thermal effects that diminish the population inversion and consequently decrease the stored energy available to amplify the pulses.

Even with a gain over 3, in order to amplify the pulses to obtain peak powers in the TW region, an amplification by a factor over 100 is needed to compensate for the system losses, mainly in the compressor, and to obtain this gain, four passes through the Cr:LiSAF crystal are necessary. The small diameter/length ratio of the Cr:LiSAF rod determines a small acceptance angle for the laser beam passages, resulting in long distances between the rod and the mirror that define the multipass amplifier geometry. The rod Brewster angled faces

reduce the acceptance angle even more due to the enlargement of the beam in the plane of incidence, in the horizontal plane in our design. To minimize this problem, we decided to restrain the four passes to the vertical plane, orthogonally to the plane of incidence defined by the Brewster faces, as schematized in figure 5. The mirror $M_2$ is located at 9 cm from one of the Cr:LiSAF faces, and mirrors $M_3$ and $M_4$ are 90 cm from the other face; the vertical separation between mirrors $M_3$ and $M_4$ is 4 mm. After being amplified by the Cr:LiSAF rod, the pulses were injected in the high-energy pulse compressor, whose losses were determined to be 43%.

The amplification results measured (with an iris between the Cr:LiSAF rod and the power meter to eliminate spontaneous emission energy) as a function of the pumping energy ($\mathcal{E}_{\text{pump}}$) are shown in table 1 and in figure 6. The final (compressed) pulse energies, $\mathcal{E}_{\text{pulse}}$, and temporal durations, $\tau_{\text{p}}$, were measured at 5 Hz repetition rate, since the amplification is the same as at 1 Hz (figure 4). The amplification $\mathcal{A}$ is shown in the upper graph on figure 6 as filled circles; the right scale indicates the measured energy of the pulses after

**Table 1.** Four-pass amplification at 5 Hz repetition rate. The pump and pulse energies are shown in the first and second columns, and the amplification in the third column. The fourth column shows the fourth power of the single-pass amplification, the fifth column exhibits the pulse duration (FWHM) measured by a single-shot autocorrelator, and the last column present the calculated peak power of the pulses.

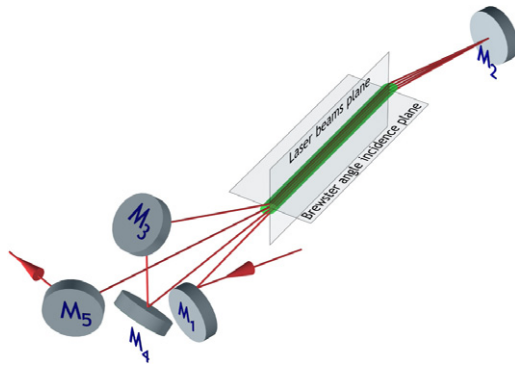| $\mathcal{E}_{pump}$ (J) | $\mathcal{E}_{pulse}$ (mJ) | $\mathcal{A}$ | $(\mathcal{A}_{1pass})^4$ | $\tau_p$ (fs) | $P$ (GW) |
|---|---|---|---|---|---|
| 0 | $0.174 \pm 0.007$ | $1.00 \pm 0.06$ | 1 | $49.9 \pm 0.2$ | $3.5 \pm 0.1$ |
| 20 | $0.47 \pm 0.1$ | $2.67 \pm 0.13$ | 2.69 | $50.1 \pm 0.2$ | $9.3 \pm 0.3$ |
| 40 | $1.54 \pm 0.05$ | $8.82 \pm 0.44$ | 9.18 | $51.0 \pm 0.2$ | $30.1 \pm 0.9$ |
| 60 | $4.5 \pm 0.2$ | $26.0 \pm 1.4$ | 27.8 | $53.4 \pm 0.2$ | $84.6 \pm 2.8$ |
| 80 | $11.4 \pm 0.4$ | $65.7 \pm 3.3$ | 72.1 | $55.5 \pm 0.2$ | $205.9 \pm 6.3$ |
| 100 | $19.0 \pm 1.0$ | $109 \pm 7$ | 170.4 | $59.8 \pm 2.0$ | $318 \pm 16$ |
| *100* | *29.7 ± 3.0* | *170.4* | *170.4* | *59.8 ± 2.0* | *496 ± 57* |



**Figure 5.** Scheme of the four-pass Cr:LiSAF amplifier geometry (the refraction angles of the beams entering and leaving the rod are not real, and the distances are not to scale). The mJ level pulses are injected in the amplifier by mirror $M_1$ in an ascendant trajectory, then mirrors $M_2$, $M_3$ and $M_4$ define the subsequent passes; after the fourth pass the pulses pass between mirrors $M_3$ and $M_4$ to mirror $M_5$ and to the compressor.



**Figure 6.** Upper graph: the filled circles represent the four-pass amplification dependence on the pumping energy, and the empty squares are the fourth power of the single-pass amplification from figure 1, with the right scale indicating the pulse energy. The lower graph shows the amplified pulses temporal pulsewidth (FWHM) after compression.

compression. In the same graph, the hollow squares represent the fourth power of the single-pass amplification results shown in figure 1, and a good agreement is observed, except for the data at the highest pumping energy (100 J). This deviation occurs because, at this higher pumping, the amplified pulse damaged the Cr:LiSAF rod and mirror $M_2$. Nevertheless, it was possible to measure the energy (30 mJ) and pulse duration (60 fs FWHM, on the single-shot autocorrelator) at the maximum pumping energy, resulting in a pulse with 0.5 TW of peak power (last line in table 1, in italics), that damaged the gain medium. The subsequent energy measurements provided the last point shown in figure 6 upper graph, with 0.3 TW of peak power (sixth line in table 1). For the temporal measurements, shown in the lower graph of figure 6, the distance between the compressor gratings was adjusted to minimize the pulsewidth at the single-shot autocorrelator when there was no pumping in the rod (unitary amplification), and was kept for the amplification measurements. This graph depicts the temporal pulsewidth (FWHM) measured along with an exponential function fitted to the five initial points. The last point, in grey, represents the value of the fitted function at the highest pumping energy with an estimated error ten times greater than measured at the lower pumping energies, and was used to estimate the peak power at 100 J pumping. Even after the damage, the peak power obtained at the higher pumping energy exceeded 0.3 TW, at 5 Hz repetition rate.
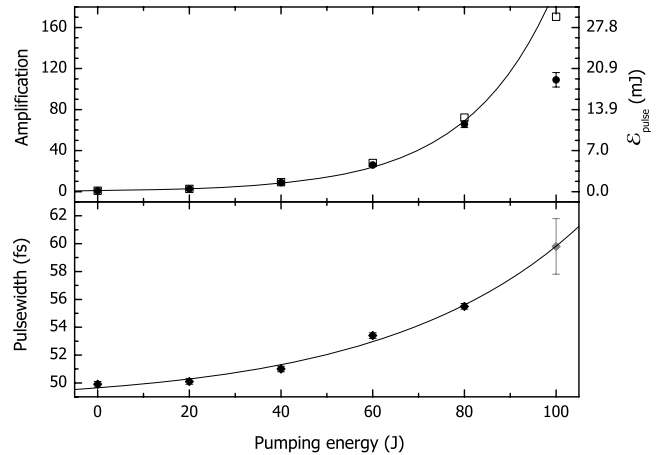
Previous results of similar peak power for this crystal were always limited to 1 Hz. It was not possible to measure the spectra of the amplified pulses before the rod was damaged, so the pulse temporal broadening can be explained, in part, by gain narrowing. However, at the higher pumping energy, we calculated a $B$ integral [23] value of 1.2, which is corroborated by the small (20%) increase in the pulse temporal width after compression, and once the distance between the gratings was not increased after the initial optimization, the pulses could have been shortened, generating higher peak powers at 5 Hz repetition rate.

Measuring the damage sizes in the Cr:LiSAF rod and in mirror $M_2$, the damages were estimated to have occurred at fluences close to 0.3 J cm$^{-2}$, five times smaller than the value we have measured for Cr:LiSAF crystals at 20 ps duration [24]. This result, together with the damage shape that occurred at two separated places (inside the beam diameter) simultaneously, indicates that the beam had hot spots with very high local intensities that damaged the optical components. Further investigation allowed determining that these hot spots were due to misalignments in the whole amplification chain, and a careful alignment aimed at improving the beam transversal profile will eliminate them.

## 4. Conclusions

We developed a Cr:LiSAF pumping cavity with reduced thermal load in the crystal rod, that could be operated as a laser or as an ultrashort pulse amplifier. Amplification over 150 was obtained, generating pulses at 5 Hz repetition rate with peak powers over 0.3 TW, the highest obtained by a laser system in the southern hemisphere. At 0.5 TW peak power the gain medium was damaged as a consequence of the presence of hot spots in the beam. At the present time we are working to improve the beam transversal energy distribution, eliminating hot spots, and also to stretch the pulses to larger pulsewidths, which will allow amplification to higher energies and peak powers in the 1 TW region. Gain narrowing in the Cr:LiSAF amplifier has to be determined to verify its influence in the final compressed pulses' temporal width. Using the presented configuration, higher repetition rates could be obtained at the expense of less amplification per pass (figure 4). Alternatively, the use of filter set 2, that results in a smaller amplification, would probably allow operation at higher repetition rates, as occurred when operating the pumping cavity as a laser resonator [21].

## Acknowledgments

## References

[1] Payne S A, Chase L L and Wilke G D 1989 Optical spectroscopy of the new laser materials, LiSrAlF$_6$:Cr$^{3+}$ and LiCaAlF$_6$:Cr$^{3+}$ *J. Lumin.* **44** 167–76

[2] Payne S A, Chase L L, Smith L K, Kway W L and Newkirk H W 1989 Laser performance of LiSrAlF$_6$:Cr$^{3+}$ *J. Appl. Phys.* **66** 1051–6

[3] Stalder M, Chai B H T and Bass M 1991 Flashlamp pumped Cr:LiSrAlF$_6$ laser *Appl. Phys. Lett.* **58** 216–8

[4] Scheps R, Myers J F, Serreze H B, Rosenberg A, Morris R C and Long M 1991 Diode-pumped Cr:LiSrAlF$_6$ laser *Opt. Lett.* **16** 820–2

[5] Agate B, Kemp A J, Brown C T A and Sibbett W 2002 Efficient, high repetition-rate femtosecond blue source using a compact Cr:LiSAF laser *Opt. Express* **10** 824–31

[6] Ihara M, Tsunekane M, Taguchi N and Inaba H 1995 Widely tunable, single-longitudinal-mode, diode-pumped CW Cr:LiSAF Laser *Electron. Lett.* **31** 888–9

[7] Uemura S and Torizuka K 1999 Generation of 12 fs pulses from a diode-pumped Kerr-lens mode-locked Cr:LiSAF laser *Opt. Lett.* **24** 780–2

[8] Shimada T, Early J W, Lester C S and Cockroft N J Repetitively Pulsed Cr:LiSAF for LIDAR Applications *Osa Proc. on Advanced Solid-State Lasers (Salt Lake City, UT, USA, 7–10 February 1994)* ed T Y Fan and B Chai **20** pp188–91

[9] Klimek D E and Mandl A 2002 Power scaling of a flashlamp-pumped Cr:LiSAF thin-slab zig-zag laser *IEEE J. Quantum Electron.* **38** 1607–13

[10] Takada H, Miyazaki K and Torizuka K J 1997 Flashlamp-pumped Cr:LiSAF laser amplifier *IEEE J. Quantum Electron.* **33** 2282–5

[11] White W E, Hunter J R, Vanwoerkom L, Ditmire T and Perry M D 1992 120 fs terawatt Ti:Al$_2$O$_3$/Cr:LiSrAlF$_6$ laser system *Opt. Lett.* **17** 1067–9

[12] Beaud P, Richardson M, Miesak E J and Chai B H T 1993 8 TW 90 fs Cr:LiSAF laser *Opt. Lett.* **18** 1550–2

[13] Ditmire T, Nguyen H and Perry M D 1995 Amplification of femtosecond pulses to 1 J in Cr:LiSrAlF$_6$ *Opt. Lett.* **20** 1142–4

[14] Payne S A, Smith L K, Beach R J, Chai B H T, Tassano J H, Deloach L D, Kway W L, Solarz R W and Krupke W F 1994 Properties of Cr:LiSrAlF$_6$ crystals for laser operation *Appl. Opt.* **33** 5526–36

[15] Stalder M, Bass M and Chai B H T 1992 Thermal quenching of fluorescence in chromium-doped fluoride laser crystals *J. Opt. Soc. Am.* B **9** 2271–3

[16] Ditmire T and Perry M D 1993 Terawatt Cr:LiSrAlF$_6$ laser system *Opt. Lett.* **18** 426–8

[17] Ditmire T, Nguyen H and Perry M D 1994 Design and performance of a multiterawatt Cr:LiSrAlF$_6$ laser system *J. Opt. Soc. Am.* B **11** 580–90

[18] Perry M D, Strickland D, Ditmire T and Patterson F G 1992 Cr:LiSrAlF$_6$ regenerative amplifier *Opt. Lett.* **17** 604–6

[19] Hanson F, Bendall C and Poirier P 1993 Gain measurements and average power capabilities of Cr$^{3+}$:LiSrAlF$_6$ *Opt. Lett.* **18** 1423–5

[20] Samad R E, Nogueira G E C, Baldochi S L and Vieira N D 2006 Development of a flashlamp-pumped Cr:LiSAF laser operating at 30 Hz *Appl. Opt.* **45** 3356–60

[21] Samad R E, Baldochi S L, Nogueira G E C and Vieira N D 2007 30 W Cr:LiSrAlF$_6$ flashlamp-pumped pulsed laser *Opt. Lett.* **32** 50–2

[22] Perry M D and Mourou G 1994 Terawatt to petawatt subpicosecond lasers *Science* **264** 917–24

[23] Perry M D, Ditmire T and Stuart B C 1994 Self-phase modulation in chirped-pulse amplification *Opt. Lett.* **19** 2149–51

[24] Samad R E, Baldochi S L and Vieira J N D 2008 Diagonal scan measurement of Cr:LiSAF 20 ps ablation threshold *Appl. Opt.* **47** 920–4